

# Temperature-dependent studies on the electrical properties of pyrolytic ZnO thin film prepared from $\text{Zn}(\text{C}_2\text{H}_3\text{O}_2)_2$

M. G. AMBIA, M. N. ISLAM

*Department of Applied Physics and Electronics, Rajshahi University, Rajshahi, Bangladesh*

M. OBAIDUL HAKIM

*Department of Physics, Rajshahi University, Rajshahi, Bangladesh*

Pyrolytically deposited transparent conducting zinc oxide thin films on glass substrates were successively subjected to a post-deposition heat treatment in air and in vacuum. The effects of heat treatment on the electrical transport properties were studied in detail. The films were polycrystalline in structure and the oxygen chemisorption–desorption process was found to play an important role in controlling the electronic properties. Various grain-boundary and energy-band parameters were calculated by taking conventional extrinsic semiconductor theory and grain-boundary trapping models into account. The samples were non-degenerative at room temperature and Hall mobility was found to be modulated by the grain-boundary potential barrier height via sample temperature.

## 1. Introduction

Polycrystalline zinc oxide thin films have attracted interest as a transparent conductive material for use in efficient energy-conversion systems. Both undoped and doped ZnO films are used in optoelectronic display devices [1] and ultra-high-frequency electroacoustic transducers [2]. In solar cells, ZnO thin films are used as transparent electrodes.

These films can be prepared on glass substrates in a number of ways of which spray pyrolysis is the simplest method. Films prepared in this way are generally polycrystalline in structure and a past history shows that the properties of these films depend very much on the deposition process. This is indeed the case, because the deposition is carried out in the open air and there always remain some uncertainties in the control of process variables in such an open atmosphere [3].

It is expected that properties of the films deposited in the open air at high temperature should respond in a distinct way to any post-deposition heat treatment after their deposition. Various chemisorption and desorption processes and oxygen-diffusion mechanisms are involved when the films are heat treated in air and also in vacuum. A successive operation of heat treatment may thus be interesting. Here, we report the effect of repeated heat treatment on the electrical properties of undoped ZnO thin films prepared in our laboratory by using a modified spray apparatus [3]. The obtained films were optically very transparent in the visible range of the spectrum.

## 2. Experimental procedure

Undoped ZnO thin films were prepared from 0.4 M

solution of  $\text{Zn}(\text{C}_2\text{H}_3\text{O}_2)_2 \cdot 2\text{H}_2\text{O}$  at various substrate temperatures (300, 330, 360 and 390 °C). The films were of similar thicknesses, 173 nm on glass substrates. The details of the film deposition process are described elsewhere [4]. After deposition, the films were cooled at a rate of  $100^\circ\text{C min}^{-1}$  and were preserved for the heat-treatment experiment. The samples were nonstoichiometric but homogeneous in structure.

Heat treatment was performed in four steps as described below. The heating and cooling rate was  $\sim 5^\circ\text{C min}^{-1}$  for each sample.

After completing the first step of heating and cooling cycle in air, the second step was performed on the sample in a similar manner to the first. Then the sample was placed in a vacuum of the order of  $10^{-5}$  torr (1 torr = 133.322 Pa) and heat treated there for the first time. It was then removed from the vacuum chamber and a third step of heat treatment was performed in air. The sample was then placed in a vacuum for the second time and heat treated. After the second vacuum heat treatment the sample was heat treated again in air for the fourth time. The successive heat-treatment operation enables the resistivity of the sample to fall to a minimum value. Electrical resistivity and Hall coefficients were measured simultaneously during heat treatment in air only. A flat nichrome wire strip heater was used to heat the sample. Starting from room temperature, the maximum heating temperature was 200 °C for all the samples. The temperature of the sample was measured by a digital thermometer (RS Components STK No. 610-067, with thermocouple Type K, UK) and for electrical measurement digital multimeters were used (Hewlett Packard 3465A).

### 3. Results and discussion

Variation of resistivity with temperature of a typical undoped ZnO sample is shown in Fig. 1. The sample is undoped in the sense that no intentional dopant has been used during deposition, but various crystal defects and impurities from the starting material may be present in the film. As observed in the figure, the heating and cooling cycles are almost irreversible in the temperature range investigated. In the first step of heat treatment, a virgin sample shows a sharp decrease in resistivity when 100°C is reached. From room temperature to 100°C, the variation in resistivity with temperature is not very significant. This type of behaviour was observed for all the samples, irrespective of their deposition temperature. In Fig. 1, BC represents the fall of resistivity up to 200°C. In the reverse cycle of cooling, CD, resistivity does not change remarkably.

In the second step of heat treatment as represented by DE, resistivity continues to fall gradually up to 130°C. The cooling cycle, EF, is similar to CD. FG represents the fall in resistivity when heat treated in vacuum at 200°C for 1 h. The third step of air heat treatment was then carried out on this vacuum-annealed sample. GH shows the variation in resistivity which still decreases slowly with temperature up to 117°C, and then shows a slightly upward tendency. The cooling cycle, HI, initially partially follows the heating cycle, HG. This cycle is thus slightly reversible. The drop in resistivity in GH is relatively smaller than that in DE. IJ shows the drop in resistivity due to

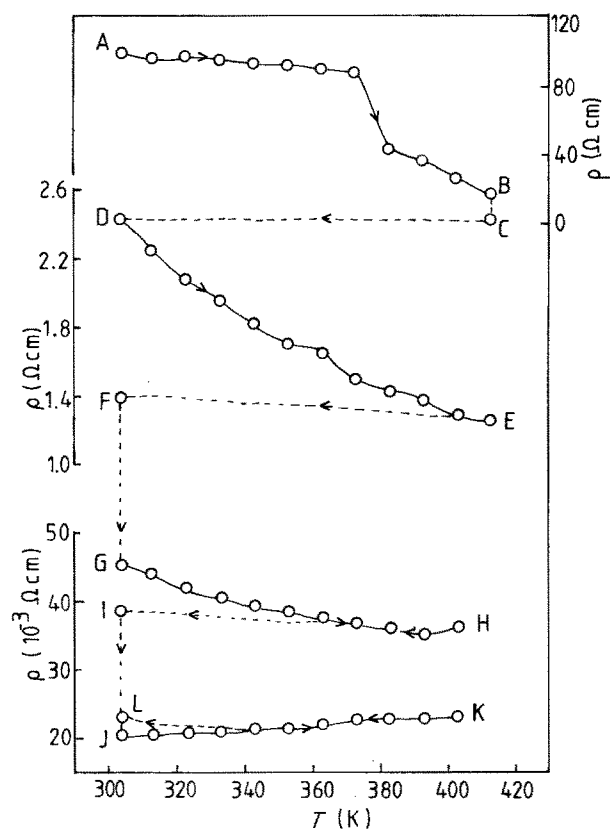


Figure 1 Variation of resistivity with temperature of a typical sample of ZnO deposited with substrate temperature of 360°C. FG and IJ represent the drop in resistivity during the first and second vacuum heat treatment, respectively.

a second vacuum heat treatment. JK shows the fourth heating cycle in air, and this time resistivity shows a slight increase with increasing temperature. The reverse cycle of cooling, KL, mostly follows the heating cycle, except in the last portion. Therefore, this cycle is also partially reversible. During the variation of resistivity,  $\rho$ , the carrier concentration,  $n$ , and Hall mobility,  $\mu$ , were also found to vary with temperature. All the samples exhibit  $n$ -type conductivity.

It is known that pyrolytically deposited film with a deposition temperature  $>250^\circ\text{C}$  is polycrystalline in structure [1, 5]. Some of our samples have been tested with a transmission electron microscope which also revealed a small-grained structure uniformly spread over the substrate surface. At the time of film deposition, because air has been used as carrier gas, it is quite likely that a large number of oxygen molecules are chemisorbed in the film at the grain boundary and on the surface during deposition, because these molecules do not have time to leave the sample at the end of deposition, due to the rapid cooling effect. It seems that in the virgin state of the film these molecules have an empirical binding energy of about 0.032 eV ( $\approx 100^\circ\text{C}$ ) which is then supplied to the sample in a post-deposition heat treatment (1st heating cycle), when the molecules begin to leave the sample rapidly and the resistivity falls. Otherwise, heating to  $100^\circ\text{C}$  and cooling is almost a reversible path without any significant change in resistivity, as was observed in another set of samples. A detailed explanation of the nature of this chemisorption on ZnO film has been given by Fujita and Kwan [6] and experimentally confirmed by Chang [7]. They mentioned that the principal chemisorption species in ZnO is  $\text{O}_2^{-1}$  at low temperature, and as the temperature of the sample rises, the chemisorbed  $\text{O}_2^{-1}$  desorbed from the sample surface donating an electron to ZnO ( $\text{O}_2^{-1} \rightarrow \text{O}_2 + e$ ), and hence the conductivity rises rapidly. The first sharp fall in resistivity above  $100^\circ\text{C}$  may thus be due to a surface effect.

The second step of heat treatment is the most significant one and we can apply the conventional semiconducting theories to calculate the various energy-band parameters for our samples.

#### 3.1. The donor ionization energy

Although the samples are undoped, they are extrinsic and polycrystalline in structure. Electrical conductivity in such a film is mainly controlled by the impurity level. The carrier concentration,  $n$ , shows a temperature dependence which can be represented by a conventional expression [8]

$$n = (n_0 N_d)^{1/2} \exp(-E_d/2k_B T) \quad (1)$$

where  $E_d$  is the donor ionization energy,  $N_d$  is the donor density and  $n_0 = 2(2\pi m_e^* k_B T/h^2)^{3/2}$ . By plotting  $\ln(nT^{-3/4})$  against  $1/T$ ,  $E_d$  can be calculated. Fig. 2 shows these plots, and the calculated values are given in Table I. The donor levels are shallow and are mainly due to the native defects, such as interstitial zinc and oxygen vacancies. Considering a hydrogenic model for the impurities, the density of states effective

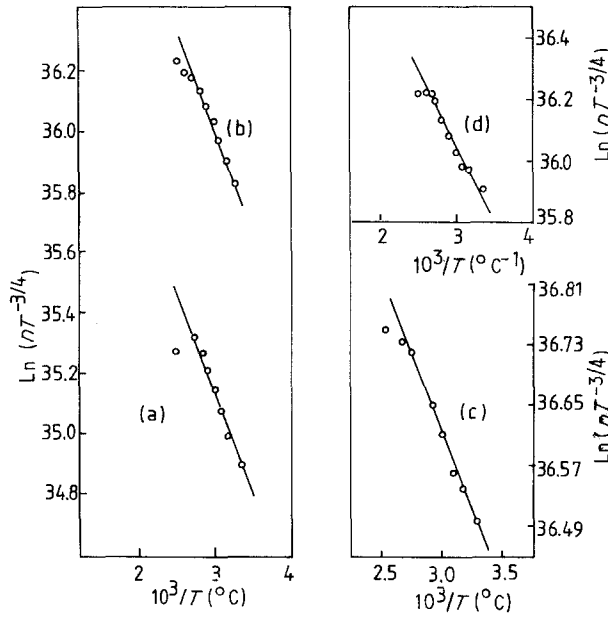


Figure 2 Plot of  $\ln(nT^{-3/4})$  as a function of  $T^{-1}$  for samples with (a)  $T_s = 300^\circ\text{C}$ , (b)  $T_s = 330^\circ\text{C}$ , (c)  $T_s = 360^\circ\text{C}$ , (d)  $T_s = 390^\circ\text{C}$ .

mass,  $m_e^*$ , can be calculated in such a material, using the relation

$$E_d = e^4 m_e^* / (2 \varepsilon^2 \hbar^2) \text{ (c.g.s)} \quad (2)$$

where  $\varepsilon$  is the dielectric constant of the medium ZnO, and can be taken from Hutson [9] as  $\varepsilon = 8.5$ . Calculated values of  $m_e^*$  are given in Table I. The position of the Fermi level of our samples can be given by [8]

$$E_F = -E_d/2 + k_B T/2 \ln[N_d h^3 / (2\pi m_e^* k_B T)^{3/2}] \quad (3)$$

The calculated values of  $E_F$  with reference to the conduction-band edge,  $E_c$ , are also given in Table I. It is noticed that the Fermi levels in all the samples lie near to but just above the donor levels, except in Sample 1 where it lies just below it.  $N_d$  is greater than  $n$  in these samples which is characteristic of an uncompensated semiconductor. In Sample 1, due to its lower deposition temperature, probably a greater number of acceptor states are present which reduces the donor density, on the one hand, and pulls the Fermi level to just below the donor level, on the other. Barnes *et al.* [10] mentioned that possible acceptor states in ZnO may arise due to the presence of chemisorbed oxygen in the grain-boundary region and may also arise from point defects such as interstitial oxygen and zinc vacancies [11], and departure from stoichiometry. However, in a thin-film polycrystalline sample, the carrier

concentration may be reduced significantly due to trapping of carriers at the grain boundary. This behaviour, as observed in Sample 1, has been termed autocompensation by Amick [12], and modelled by Bernarczyk and Bednarczyk [13].

### 3.2. Grain-boundary parameters

In polycrystalline samples the electrical properties are largely controlled by the grain-boundary effects. It can be pointed out briefly from the grain-boundary trapping models [14, 15] that when the trapping states in the grain-boundary region are occupied they create a depletion region in the grain and a potential barrier at the interface. Under this situation, if the grain size,  $l$ , is larger than twice the Debye screening length,  $L_D$ , then the measured mobility,  $\mu$ , is thermally activated with an activation energy,  $\phi_b$ , which is the barrier height at the grain boundary [14]. In an extrinsic non-degenerate sample, thermally activated mobility can be accounted for by [15]

$$\mu = \mu_0 T^{-1/2} \exp(-\phi_b/k_B T) \quad (4)$$

where

$$\mu_0 = el/(8\pi m_e^* k_B)^{1/2} \quad (5)$$

is a constant which depends on grain size,  $l$ . In our sample, the carrier concentrations are of the order of  $\sim 10^{17} \text{ cm}^{-3}$ , and the position of the Fermi level indicates that the samples are non-degenerate. Plotting  $\ln(\mu T^{1/2})$  as a function of  $1/T$ ,  $\phi_b$  can be determined. Fig. 3 shows such plots where we can see that the mobility is thermally activated in the investigated temperature range. Calculated values of  $\phi_b$  are given in Table II.

#### 3.2.1. Grain-size estimation

Taking Equation 5 into consideration, and using the measured values of mobilities and  $\phi_b$  at room temperature, the grain size,  $l$ , can be estimated, but it would not be of the expected order, because Equation 4 is strictly valid when the mobility is mainly dominated by the grain boundaries. A corrected value of  $\mu_0$  can be obtained by using  $\mu_g$  in place of  $\mu$  in Equation 4 where the approximation in Equation 6 is taken as valid by Matthiessen's rule

$$1/\mu = 1/\mu_g + 1/\mu_s \quad (6)$$

where  $\mu_g$  is the grain-boundary limited mobility, and  $\mu_s$  is the corresponding value of mobility if the sample were single crystal having the same structure as the

TABLE I Various parameters of interest for ZnO thin film

Sample	Substrate temperature, $T_s$ ( $^\circ\text{C}$ )	Resistivity ( $\Omega \text{ cm}$ )	Carrier conc. in the grain, $n_1 = n$ ( $10^{17} \text{ cm}^{-3}$ )	Donor ionization energy, $E_d$ (eV)	Fermi level, $E_F$ (eV)	Donor density, $N_d$ ( $10^{17} \text{ cm}^{-3}$ )	Effective mass, $m_e^*/m_e$	TCR ( $10^{-3} \text{ }^\circ\text{C}^{-1}$ )
1	300	14.49	1.09	0.112	0.12	0.921	0.59	-5.07
2	330	11.03	2.67	0.113	0.10	4.3	0.60	-4.01
3	360	2.44	5.14	0.069	0.061	7.5	0.36	-4.42
4	390	3.13	2.86	0.079	0.075	4.63	0.42	-4.67

film. For approximation, the bulk value of  $\mu$  can be taken for  $\mu_s$ . We have taken  $\mu_s$  from the intercept of a  $\mu$  versus  $1/t$  plot where  $t$  is the film thickness, Fig. 4. The calculated values of grain size,  $l$ , are shown in Table II, and are of the expected order of magnitude. This shows that a higher deposition temperature favours relatively larger grain formation, which agrees well with the TEM observations.

### 3.2.2. Debye screening length

A hydrogenic model for the possible donor centres enables the Debye screening length [8] to be calculated from

$$1/L_D^2 = 4n^{1/3}/a_0 \text{ (c.g.s.)} \quad (7)$$

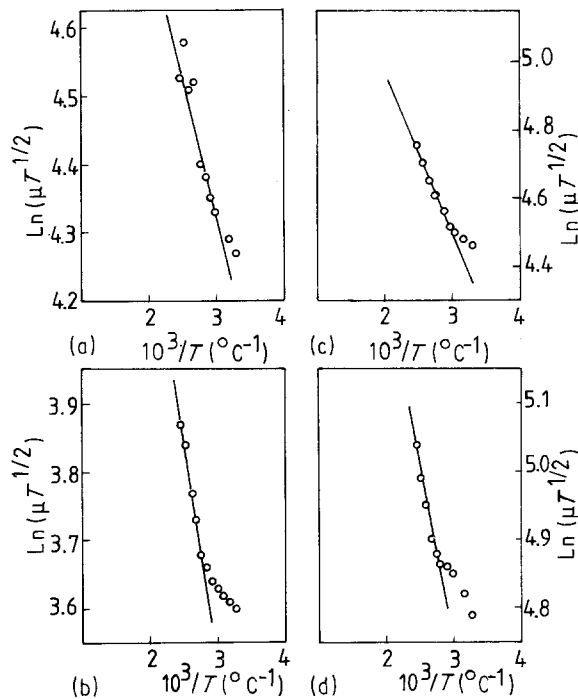


Figure 3 Plot of  $\ln(\mu T^{1/2})$  as a function of  $T^{-1}$  for samples with (a)  $T_s = 300^\circ\text{C}$ , (b)  $T_s = 330^\circ\text{C}$ , (c)  $T_s = 360^\circ\text{C}$  and (d)  $T_s = 390^\circ\text{C}$ .

where  $n$  is the uniform carrier concentration and  $a_0$  is the Bohr radius for the donor centres, given by

$$a_0 = \epsilon \hbar^2 / m_c^* e^2 \quad (8)$$

Using Equation 8 in Equation 7 we obtain

$$L_D = (\hbar/2e)(m_c^* n^{1/3}/\epsilon)^{-1/2} \quad (9)$$

Calculated values of  $L_D$  using Equation 9 for our samples are given in Table II. It is noticed that the condition  $2L_D < l$  of a trapping model is correctly obeyed here. Thus our approach of analysing the data by using the grain-boundary trapping model for the thermal activation of mobility, is valid.

The effect of the successive heat treatment on the samples is briefly given in Table III. Because of the heat treatment, the resistivity of all the samples has been lowered drastically, by more than 99%. The Hall mobility in the virgin sample was relatively difficult to measure; values given in Table III are the results of several observations, but may still be approximate. A large change in Hall mobility occurs in films deposited at lower substrate temperature. In all cases mobility was found to increase due to heat treatment. The

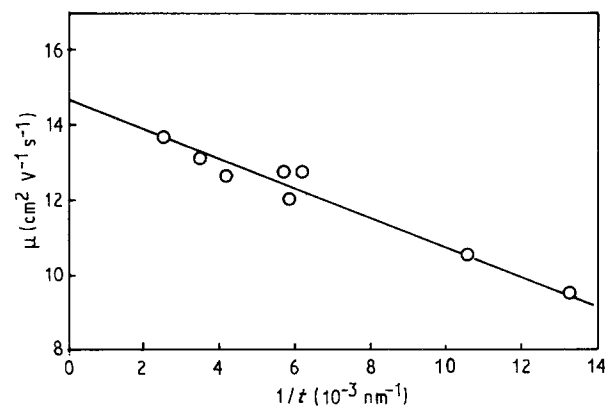


Figure 4 Variation of Hall mobility,  $\mu$ , with inverse of film thickness,  $t$ , (all samples are heat treated).

TABLE II Various grain-boundary parameters of polycrystalline ZnO thin film

Sample	Deposition temperature, $T_s$ ( $^\circ\text{C}$ )	Hall mobility, $\mu$ ( $\text{cm}^2 \text{V}^{-1} \text{s}^{-1}$ )	Grain boundary barrier height, $\phi_b$ (eV)	Interface trap density, $N_t$ ( $10^{11} \text{cm}^{-2}$ )	Carrier conc. in the barrier region, $n_2$ ( $10^{16} \text{cm}^{-3}$ )	Estimated grain size, $l$ (nm)	Debye screening length, $L_D$ (nm)	Mean free path, $L$ (nm)
1	300	4.14	0.036	3.84	2.58	3.6	1.37	0.296
2	330	2.12	0.051	7.156	3.47	2.9	1.17	0.128
3	360	4.96	0.040	8.79	10.3	4.3	1.57	0.30
4	390	6.95	0.045	6.95	4.72	10.0	1.54	0.575

TABLE III The effect of successive heat treatment on  $\rho$ ,  $\mu$  and  $n$

Sample	Resistivity in the virgin state ( $\Omega \text{cm}$ )	Min. resistivity attained ( $\Omega \text{cm}$ )	Percentage change (drop) (%)	Hall mobility in the virgin state ( $\text{cm}^2 \text{V}^{-1} \text{s}^{-1}$ )	Max. mobility attained ( $\text{cm}^2 \text{V}^{-1} \text{s}^{-1}$ )	Percentage change (increase) (%)	Carrier conc. in the virgin state ( $10^{15} \text{cm}^{-3}$ )	Max. conc. attained ( $10^{18} \text{cm}^{-3}$ )	Increase in order of magnitude
1	96.65	0.223	99.77	4.1	15.9	288	2.6	1.75	$10^3$
2	98.78	0.086	99.91	4.4	11.29	157	13.3	6.32	$10^2$
3	101.2	0.02	99.98	4.8	12.8	167	8.79	28.8	$10^4$
4	30.3	0.058	99.8	6.9	12.4	80	4.02	3.67	$10^3$

carrier concentration also increases by several orders of magnitude, although in the virgin film it was hard to measure. In the fourth step of heat treatment the nature of the variation of resistivity, Hall mobility and carrier concentration with temperature is almost flat, which indicates that desorbable oxygen is exhausted from the sample and the film is relatively stable towards heat treatment.

In fact, in a polycrystalline oxide semiconductor, oxygen chemisorption and desorption may both occur at all temperatures when heat treated in air. Which process is dominant is determined by their respective rates which are functions of the ambient temperature and relative concentrations of the chemisorption species available in the ambient and in the chemisorption sites [16]. Thus, up to the third step of heat treatment, the gross decrease in resistivity in the film is due to the oxygen desorption process which lowers the grain-boundary barrier heights, and enhances the mobility and carrier concentration. It seems that in the fourth step, chemisorption again started dominating, because the sample in hand is already exhausted of desorbable oxygen.

#### 4. Conclusions

Oxygen chemisorption-desorption processes in polycrystalline ZnO thin film are important due to their power to control the electronic transport properties. When these films are deposited by a spray pyrolysis process in air, many oxygen molecules from the atmosphere are chemisorbed in the grain boundaries and also on the surface of the film during the deposition. This produces very high resistivity of the film in the virgin state when they are undoped. When these films are heat treated in vacuum or in normal atmosphere, desorption takes place which drastically increases the electrical conductivity, Hall mobility and carrier concentration. Hall mobility is controlled by the grain-boundary potential barrier heights which are modulated by the heat-treatment effects. In the undoped sample, the possible donor levels are shallow

and are situated at various depths in the band gap. Fermi levels lie near the donor levels, but are at  $2.4\text{--}4.8 k_B T$  below the conduction band edge at room temperature. The samples are thus safely considered to be non-degenerate. To obtain low resistivity, successive heat-treatment operations can be performed without any deterioration of the film structure.

#### Acknowledgement

Mr M. G. Ambia thanks the U.G.C. for the financial support of the research.

#### References

1. K. L. CHOPRA, S. MAJOR and D. K. PANDYA, *Thin Solid Films* **102** (1983) 1.
2. F. S. HICKERMELL, *Proc. IEEE* **64** (1976) 631.
3. M. N. ISLAM and M. O. HAKIM, *J. Phys. Chem. Solids* **46** (1985) 339.
4. M. N. ISLAM, M. O. HAKIM and H. RAHMAN, *J. Mater. Sci.* **22** (1987) 1379.
5. S. K. GHANDHI, R. J. FIELD and J. R. SHEALY, *Appl. Phys. Lett.* **37** (1980) 449.
6. Y. FUJITA and T. KWAN, *J. Res. Inst. Catal.* **7** (1959) 24.
7. SHIH-CHIA CHANG, *J. Vac. Sci. Technol.* **17** (1980) 366.
8. C. KITTEL, "Introduction to Solid State Physics" 4th Edn (Wiley, New York, 1971) pp. 278, 373, 376.
9. A. R. HUTSON, *Phys. Rev.* **108** (1957) 222.
10. J. O. BARNES, D. J. LEARY and A. G. JORDAN, *J. Electrochem. Soc.* **127** (1980) 1636.
11. A. P. ROTH and D. F. WILLIAMS, *J. Appl. Phys.* **52** (1981) 6685.
12. J. A. AMICK, *RCA Rev.* **20** (1959) 753.
13. D. BERNARCZYK and J. BEDNARCZYK, *Thin Solid Films* **44** (1977) 137.
14. J. W. ORTON and M. J. POWELL, *Rep. Progr. Phys.* **43** (1980) 1263.
15. L. L. KAZMERSKI, "Polycrystalline and Amorphous Thin Film and Devices" (Academic Press, New York, 1980).
16. M. N. ISLAM and M. O. HAKIM, *J. Phys. D Appl. Phys.* **19** (1986) 615.

Received 17 September 1991

and accepted 2 September 1992